

Received June 28, 2020, accepted July 27, 2020, date of publication July 30, 2020, date of current version August 20, 2020.

Digital Object Identifier 10.1109/ACCESS.2020.3012978

Study on Surface Rainwater and Arc Characteristics of High-Voltage Bushing With Booster Sheds Under Heavy Rainfall

LIN YANG¹, (Member, IEEE), ZHIQIANG KUANG¹, YIJIE SUN¹, YIFAN LIAO^{1,2},
YANPENG HAO¹, (Member, IEEE), LICHENG LI¹, AND FUZENG ZHANG¹

¹School of Electric Power, South China University of Technology, Guangzhou 510640, China

²Electric Power Research Institute, China Southern Power Grid, Guangzhou 510080, China

Corresponding author: Yanpeng Hao (yphao@scut.edu.cn)

This work was supported in part by the Smart Grid Joint Fund Key Project between National Natural Science Foundation of China and State Grid Corporation under Grant U1766220 and in part by the Science and Technology Project of China Southern Power Grid under Grant CSGTRC-K163024.

ABSTRACT The flashover performance of insulators can be improved by BS (booster sheds) in the rain, which is mainly attributed to the reasons that BS break up long cascades of water and block connections of arcs. However, surface rainwater characteristics and arc characteristics of bushing have not been quantitatively studied under heavy rainfall. In this article, the artificial rain tests were conducted on a 500 kV transformer high-voltage bushing equipped with and without BS under the rainfall intensity of 10 mm/min. X (the total length of water column) and L_{arc} (the critical length of arc) on the bushing surface were taken as the feature parameters of surface rainwater characteristics and arc characteristics, respectively. The effects of BS on E_h (the rain flashover voltage gradient along the insulation height), X and L_{arc} were investigated, respectively. Furtherly, the relationships were studied among E_h , X and L_{arc} . Results indicate that E_h has a sharp rise as the number of BS (N_{BS}) is from one to two, however the rise of E_h gradually decreases when N_{BS} exceeds two. X decreases while L_{arc} increases with the rise of N_{BS} , however both the change ranges of them continually fall. Furthermore, L_{arc} presents remarkable negative correlation to X because of the effect of the electric field. E_h rises nonlinearly with the decrease of X , which is due to the change of the wetting uniformity on the bushing surface and the potential redistribution along air gaps in the presence of the local arc.

INDEX TERMS Rain flashover, booster sheds, bushing, insulation performance.

I. INTRODUCTION

The rain flashovers of insulators often occurred in the power system, which threatened power system security severely [1]–[3]. According to the statistics of flashover accidents in the Nelson River converter station from 1975 to 2013, the rain flashovers accounted for about half of the total and the most of them happened on the bushings [4]. As for the external insulation flashovers in ± 500 kV DC converter stations in China, the rain flashovers accounted for about 60% [5]. Besides, the rain flashovers have also been reported in the external insulation flashover accidents

The associate editor coordinating the review of this manuscript and approving it for publication was Mehdi Bagheri¹.

in 500 kV AC substations and become one of the main factors that affect the operation safety of EHV equipment in the power system.

There were a host of experimental researches on the prevention approaches for the rain flashovers on the external insulation of power equipment. Results showed that the flashover voltages of insulators could be raised by installing booster sheds (BS). Orsino *et al.* found that the flashover voltage of 800 kV post insulator with 3-6 BS (spacing distance of 700 mm) was 18%-24% higher than that without BS under rain of 5 mm/min [6]. Yu *et al.* performed the tests on the 500 kV porcelain bushing with 4 and 8 BS (spacing distance of 1165 and 580 mm) and found the maximum withstand voltage increased by 72.7% and 127.3%,

respectively, compared with that without BS under rain of 10 mm/min [7]. A recent study by Liu *et al.* indicated that the flashover voltage of 110 kV porcelain post insulator with 3 BS (spacing distance of 400 mm) was 26.5% higher than that without BS under rain of 2 mm/min [8].

Furthermore, many qualitative studies have been carried out on the reasons why the rain flashover voltage of insulator was improved by BS. According to the study by Ely *et al.*, there were three possible reasons for the insulation performances of post insulator and bushing improved by booster sheds under rain of 0.3-4.3 mm/min as follows: prevention of the bypassing of leakage path by cascading water, inhibition of discharge development and suppression of discharges running between booster sheds and skirts [9]. However, Lambeth *et al.* thought that the most important effect of booster sheds might be to hinder the development of the surface arc of the wall bushing, rather than shield the rainwater under non-uniform rain of 6.5 mm/min [10]. A study by Xu *et al.* indicated that under the rain of 3 mm/min, the effects of booster sheds were to separate the rainwater flowing and to avoid excessive rainwater bridging the air gap between the skirts [11]. Yu *et al.* found booster sheds can greatly improve the withstand voltage of bushing under rain of 10 mm/min because of breaking the formation of the rain streams and blocking the connection of the arcs [7].

As for the studies mentioned above, it was found that the effects of booster sheds were not exactly the same under different conditions, and the rainfall intensities were no more than 10 mm/min in the most of experiments. These studies qualitatively indicated that the booster sheds could break up long cascades of water and block the arc propagation. However, there are no quantitative analyses on the rain or arc characteristics of the high-voltage bushing. Besides, the relationships have not been explored among the rain flashover voltage, surface rainwater characteristics and arc characteristics.

In this article, the artificial rain tests are carried out on a 500 kV transformer high-voltage bushing equipped with and without booster sheds under the rainfall intensity of 10 mm/min. In order to quantitatively investigate the effects of booster sheds on the rain flashover voltage, surface rainwater characteristics and arc characteristics of the bushing, the total length of water column and the critical length of arc are taken as the feature parameters of surface rainwater characteristics and arc characteristics, respectively. Furthermore, the relationships among the rain flashover voltage, surface rainwater characteristics and arc characteristics are revealed, which contributes to explain the mechanism of the rain flashover voltage raised by installing booster sheds.

II. TEST ARRANGEMENT

A. EXPERIMENTAL SET-UP

The schematic diagram of the experimental set-up is shown in Fig. 1. AC high voltage through the wall bushing was led to the test sample vertically locating in the climate chamber.

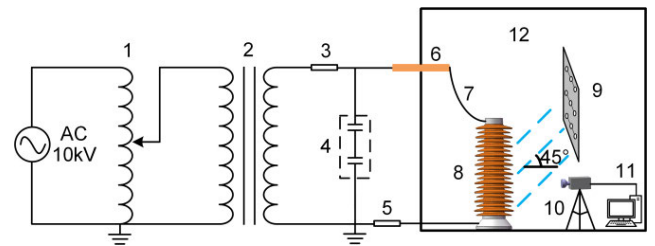


FIGURE 1. Schematic diagram of the experimental set-up. (1) voltage regulator; (2) transformer; (3) protective resistor; (4) ac voltage divider; (5) leakage current measuring sensor; (6) wall bushing; (7) high voltage line; (8) test bushing; (9) rain shelf; (10) camera; (11) computer; (12) climate chamber.

In Fig. 1, the AC power supply system was composed of 10 kV, 3000 kVA post voltage regulator, 450 kV, 2700 kVA high-voltage test transformer and 450 kV AC capacitor voltage divider. The relevant indicators met the requirements of standard IEC 60507 [12].

The climate chamber was 16 m × 12 m × 16 m in size. The rain shelf, consisting of 5 × 20 nozzle arrays, was 12m high, and each nozzle can be independently controlled to adjust rainfall.

In order to study surface rainwater characteristics, a Canon 5D camera was adopted to take photos of the rain condition on bushing in the artificial rain. No less than eight consecutive photos with the interval time of 125 ms were taken to reduce the data dispersion. With the purpose of investigating arc characteristics, a Vision Research Phantom 12.1 high-speed camera at the shooting speed of 1000 frames/s was used to record the process of arc propagation on the bushing surface in the tests.

B. TEST SAMPLE AND CONDITION

In this article, the bottom half of a 500 kV transformer porcelain bushing was selected as the test sample with a single large and small shed configuration, and the sample parameters were shown in Table 1.

TABLE 1. Parameters of the sample.

Insulation height	Leakage distance	Large shed Spacing	Large shed overhangs	Difference between large and small shed overhangs	Average rod diameter
2380 mm	9950 mm	70 mm	71 mm	25 mm	465 mm

In the tests, both the horizontal and vertical components of rain were 10 mm/min to simulate the natural heavy rain. The rainfall angle was 45° to simulate a windy environment, and rainwater conductivity was 300 μS/cm. The sample surface was coated by pollution layer with the salt deposit density (SDD) of 0.06 mg/cm² and the non-soluble deposit density (NSDD) of 0.36 mg/cm².

The rain flashover tests on the sample equipped without BS and with 1-4 BS were carried out. According to China

electric power industry standard DL/T 1469 [13], the first booster shed was installed on the third large shed under the high-voltage wire. When the number of booster sheds (N_{BS}) was more than one, BS were positioned uniformly along the sample, as shown in Fig. 2.

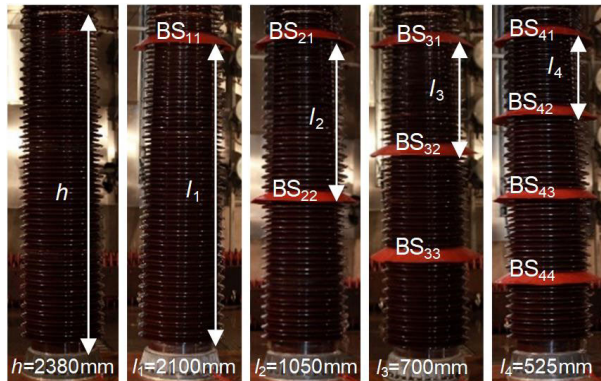


FIGURE 2. The sample equipped with and without Booster sheds.

In Fig. 2, BS_{mn} was the label of booster shed installed on the sample. For instance, BS_{32} was the second booster shed from top to bottom of the sample when N_{BS} was 3. h was the insulation height of the sample and l_1 was the height from BS_{11} to the grounding end. l_2 , l_3 , and l_4 were the spacing distances of 2, 3, and 4 BS, respectively.

C. TEST PROCEDURES

1) PROCEDURES OF FLASHOVER TEST

The constant voltage up-and-down method [14] was adopted for the tests, and the test procedures were as follows:

a) The sample was washed clean and dried at room temperature, and then the solid layer method [12] was applied to contaminate the sample surface.

b) 75% of the predetermined voltage U_i was applied for a while, and then rose to U_i at the range of about 2% of U_i per second. The voltage was kept at U_i constantly after that.

c) The rain device started up after the test voltage U_i maintained for 5 min. If flashover did not occur within 15 min, the test was stopped.

d) Returned to step a) for the next test. If flashover occurred in the last test, U_i in b) should be reduced by 5%, otherwise raised by 5%.

The sample needed to be contaminated again after cleaned no matter flashover occurring or not in the last test, and ten useful tests were required at least. The rain flashover voltage ($U_{50\%}$) and its relative standard deviation error (σ) can be calculated as follows [15], [16]:

$$U_{50\%} = \frac{1}{N} \sum (n_i \times U_i) \quad (1)$$

$$\sigma = \frac{1}{U_{50\%}} \sqrt{\frac{\sum_{i=1}^N (U_i - U_{50\%})^2}{N - 1}} \times 100\% \quad (2)$$

where U_i is an applied voltage level and n_i is the number of groups of tests carried out at the same applied voltage level; N is the number of useful tests; $N = 10$.

Furthermore, the rain flashover voltage gradient along the insulation height (E_h) can be gained by the following formula [17], [18]:

$$E_h = U_{50\%}/h \quad (3)$$

2) PROCEDURES OF SURFACE RAINWATER CHARACTERISTICS TEST

a: SELECTION OF FEATURE PARAMETER OF SURFACE RAINWATER CHARACTERISTICS

The rainwater accumulated on the edge of the bushing shed will form a water column under the effects of gravity and surface tension. Generally, the water column does not bridge the next shed and there is a “water column—air gap” between two adjacent sheds [19]. The streamer discharge [20] and the streamerlike discharge [21], across the tip of the droplets and water runnels hanging on insulator shed, develop in the air gap between the sheds. Therefore, this article photographed the discharge paths between bushing sheds as shown in Fig. 3.

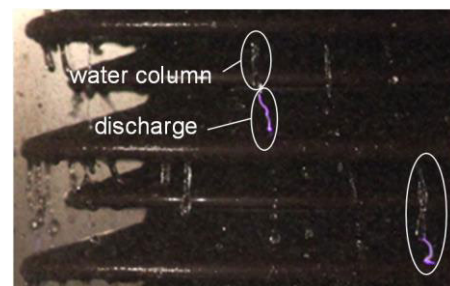


FIGURE 3. Breakdown of the air gap at the end of water column.

Fig. 3 shows that the discharge on the bushing surface started from the breakdown of the air gap at the end of the water column, which is in agreement with the studies on arc propagation in [22], [23]. The experimental phenomenon demonstrates that the length of the water column hanging on the shed edge plays a very important role in the whole process of the discharge.

Consequently, in order to quantitatively explore the relationship between surface rainwater characteristics and arc characteristics, the length of water column between two large sheds is used to characterize surface rainwater characteristics. In this article, the water column refers to the water drop which is elongating and about to break up according to [22]. Finally, the total length of water column, which can reflect the overall rain situation on the bushing surface, is taken as the feature parameter of surface rainwater characteristics.

b: MEASUREMENT OF THE TOTAL LENGTH OF WATER COLUMN

The shape of water column hanging at the edge of shed is so random that it may be vertical or sloping. Therefore,

the vertical distance from the edge of the large shed to the end of water column is taken as the length of water column, which is denoted as x , as shown in Fig. 4.

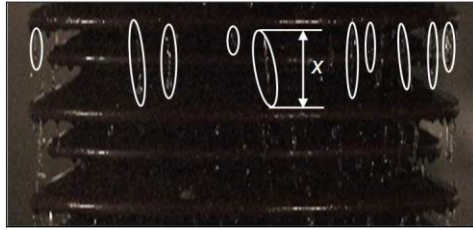


FIGURE 4. Measurement of the length of water column.

The sample has 32 large shed units named S_1 - S_{32} from top to bottom. S_1 represents the shed unit where the high-voltage wire is located, and S_{32} is the shed unit closest to the grounding end. The length of water column (x_i) can be calculated by the following formula:

$$x_i = \frac{1}{N} \sum_{j=1}^N x_{ij} = \frac{1}{N} \sum_{j=1}^N \left(\frac{1}{M} \sum_{k=1}^M x_{ijk} \right) \quad (4)$$

where j is the order number of the tests and k is the order number of the photos in one test; x_{ijk} is the average length of all water columns of the shed unit S_i in the k -th photo of the j -th test; x_{ij} is the average length of water column for M consecutive photos of the j -th test; N is the number of repeated experiments; $M = 8$ and $N = 3$.

Therefore, the total length of water column (X) on the sample surface can be gained as follows:

$$X = \sum_{i=1}^{N_{sh}} x_i \quad (5)$$

where N_{sh} is the number of shed units of the sample, $N_{sh} = 32$.

The relative standard deviation error (σ_i) is employed to represent the dispersion of x_i . Based on the Bessel formula [24], σ_i can be derived as follows:

$$\sigma_i = \frac{1}{x_i} \sqrt{\frac{\sum_{j=1}^N (x_{ij} - x_i)^2}{N - 1}} \quad (6)$$

Similarly, the relative standard deviation error of X (σ_X) can be calculated by the following equation:

$$\sigma_X = \frac{1}{X} \sqrt{\frac{\sum_{j=1}^N \left(\sum_{i=1}^{N_{sh}} x_{ij} - X \right)^2}{N - 1}} \quad (7)$$

3) PROCEDURES OF ARC CHARACTERISTICS TEST a: SELECTION AND DETERMINATION OF FEATURE PARAMETER OF ARC CHARACTERISTICS

References [7] and [9] pointed out that the booster sheds can hinder the arc propagation and increase the difficulty

in the connection of the partial arcs. However, there was no discussion about which feature parameter was involved in the arc propagation. Based on the Obenaus pollution flashover model, reference [25] derived the relationship between the arc length and the minimum voltage required to maintain the arc. The voltage required to maintain the arc dramatically dropped once the arc length exceeded the critical length of arc, which led to an inevitable flashover. Therefore, this article selects the critical length of arc [26], [27] as the feature parameter of arc characteristics to explore the effects of booster sheds on the arc propagation.

According to reference [25], the flashover occurred immediately after the arc suddenly developed downward rapidly. So, the arc propagation velocity (v) was measured through recording the arc propagation process by a high-speed camera. Therefore, the length of the arc corresponding to the moment when v started to change from low to high was defined as the critical length of arc (L_{arc}).

During the arc propagation process as shown in Fig. 5, s is the vertical distance of the downward propagation path in the period of t_1 to t_2 . Taking the arc propagation direction from the HV end to the grounding end as the positive, v within Δt ($\Delta t = t_1 - t_2$) can be calculated by the equation:

$$v = \frac{s}{t_2 - t_1} = \frac{s}{\Delta t} \quad (8)$$

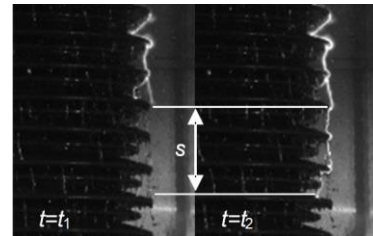


FIGURE 5. The calculation method of the arc propagation velocity.

b: MEASUREMENT OF THE CRITICAL LENGTH OF ARC

Complex thermal forces [28]–[30] and some random environmental forces can cause the arc forming an irregular shape, which makes it difficult to measure the arc length accurately [31]. The test phenomenon in this article shows that most of partial arcs develop along the axial direction, and there is almost no arc on the surface of BS before flashover.

In order to measure the arc length conveniently, the length in the vertical direction is taken as the local arc length in this article. Therefore, L_{arc} is the sum of the lengths of local under BS at the critical moment.

III. TEST RESULTS AND ANALYSES

A. RESULTS AND ANALYSES OF FLASHOVER TEST

The results of flashover test are presented in Table 2. The increase range of E_h is the percentage of the ratio between $E_{hm} - E_{hn}$ and E_{hn} , and it can effectively reflect the change of E_h with the increase of N_{BS} .

TABLE 2. The results of flashover test.

N_{BS}	0	1	2	3	4
l (mm)	-	-	1050	700	525
$U_{50\%}$ (kV)	112.4	156.2	281.6	310.6	330.2
E_h (kV/m)	47.2	65.6	118.3	130.5	138.7
$(E_{hm}-E_{hn})/E_{hn}$ (%)	-	39	80	10	6
σ (%)	4.5	2.9	4.0	2.4	3.0
$(E_{hm}-E_{h0})/E_{h0}$ (%)	-	39	150	176	194

Notes: l is spacing distance of BS (booster sheds); E_{hm} and E_{hn} are the flashover voltage gradient when N_{BS} are m and n , respectively; $n = m - 1$ ($m = 1,2,3,4$); E_{h0} is the flashover voltage gradient when N_{BS} is zero.

Based on the test results in Table 2, the relationships between N_{BS} and E_h and the increase range of E_h are obtained as shown in Fig. 6.

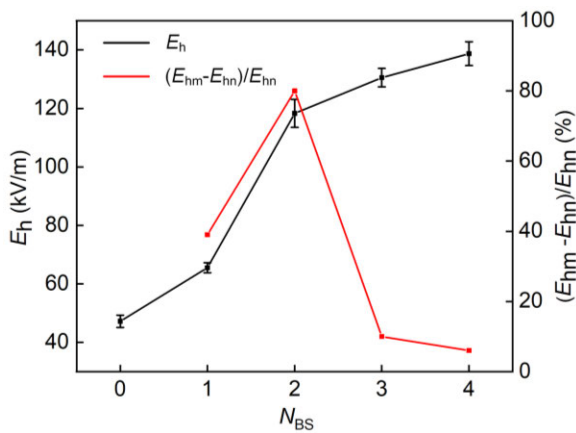
**FIGURE 6.** The relationships between N_{BS} (the number of BS) and E_h (the rain flashover voltage gradient) and the increase range of E_h .

Table 2 and Fig. 6 show that:

1) Compared with that without BS, E_h of the sample with 1-4 BS increases by 39%, 150%, 176% and 194%, respectively, which indicates that BS can effectively improve the flashover performance of the sample under heavy rainfall.

2) When N_{BS} exceeds two, the increase range of E_h gradually decreases and is no more than 10%. That is to say, E_h of the sample appears to grow with saturation as N_{BS} continuously increase.

B. RESULTS AND ANALYSES OF SURFACE RAINWATER CHARACTERISTICS TEST

The measured results of x_i , X and σ_X are listed in Table 3, and the distributions of x_i and σ_i along the bushing shed unit S_i are shown in Fig. 7.

The results in Table 3 and Fig. 7 indicate:

a) σ_i concentrates upon 4%-10% and σ_X is no more than 8%, which means that the precision of the measured results with low dispersion is satisfactory.

b) There is almost no water column between large sheds of the first three shed units under each booster shed, which is visible in the photos of the partial rain situation of the sample as shown in Fig. 8. Moreover, x_i under BS is generally rising.

TABLE 3. The results of the surface rainwater characteristics test.

N_{BS}	0	1	2	3	4
x_1	33.9	34.7	34.6	32.6	33.5
x_2	35.1	33.9	34.1	35.4	34.6
x_3	35.3	0	0	0	0
x_4	35.6	0	0	0	0
x_5	36.0	0	0	0	0
x_6	37.6	22.6	16.0	18.0	15.0
x_7	39.0	24.3	25.4	23.0	24.0
x_8	38.8	32.0	30.1	29.3	30.8
x_9	39.1	33.3	33.6	31.4	31.7
x_{10}	39.5	32.9	32.0	34.7	31.6
x_{11}	40.1	33.6	35.2	33.6	0
x_{12}	41.2	32.6	30.6	33.8	0
x_{13}	40.8	36.2	36.5	34.8	0
x_{14}	40.4	36.2	33.1	0	24.5
x_{15}	41.0	37.4	37.3	0	27.4
x_{16}	42.1	38.0	39.0	0	29.5
x_{17}	42.5	38.4	38.6	20.7	31.5
x_{18}	42.9	39.4	39.9	24.5	32.8
x_{19}	42.5	39.9	0	28.5	0
x_{20}	43.0	40.2	0	32.0	0
x_{21}	44.3	39.5	0	34.3	0
x_{22}	43.6	39.8	29.6	37.1	24.4
x_{23}	43.6	40.4	32.8	38.6	26.3
x_{24}	44.0	40.9	33.0	0	28.0
x_{25}	45.5	40.6	33.6	0	29.6
x_{26}	46.2	41.3	34.0	0	30.2
x_{27}	45.3	40.8	34.5	23.6	0
x_{28}	45.0	41.5	35.9	27.7	0
x_{29}	44.6	41.2	36.5	30.0	0
x_{30}	45.5	42.3	36.1	31.4	26.1
x_{31}	45.9	42.5	37.5	32.1	28.0
x_{32}	46.6	43.2	38.2	32.8	28.9
X	1326.5	1079.6	877.7	699.9	568.4
σ_X	4.4	5.1	6.3	6.5	7.3

Notes: mm(millimeter) is the unit of x_i and X ; % is the unit of σ_X .

c) Generally, x_i under BS decreases compared with that without BS, and the closer to BS S_i is, the greater is decrease in x_i .

According to the test results in Table 3, the relationship between X and N_{BS} is shown in Fig. 9.

Fig. 9 shows that X decreases with the increase of N_{BS} while the decrease range of X gradually falls. It is because booster sheds play an important role in sheltering rainwater and breaking up long cascades. However, as N_{BS} increases, the accumulation of rainwater on the sample sheds surface decreases gradually, leading to the falling of the decrease range of X .

C. RESULTS AND ANALYSES OF ARC CHARACTERISTICS TEST

Fig. 10 shows the results of arc propagation velocity (v) in 100 ms before flashover without BS and with 1-4 BS installed, and the critical arcs are shown in Fig. 11.

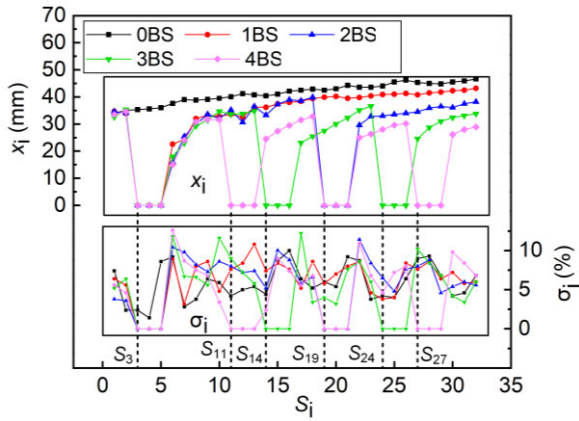


FIGURE 7. The distributions of x_i (the length of water column) and its relative standard deviation error (σ_i) along the bushing shed unit S_i : (S_3 : where BS_{11} , BS_{21} , BS_{31} and BS_{41} installed on; S_{11} : where BS_{42} installed on; S_{14} : where BS_{32} installed on; S_{19} : where BS_{22} and BS_{43} installed on; S_{24} : where BS_{33} installed on; S_{27} : where BS_{44} installed on).

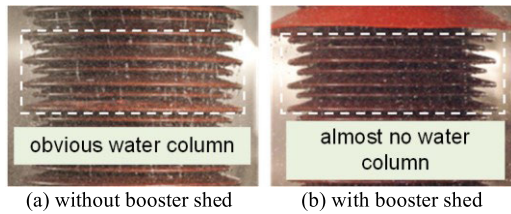


FIGURE 8. The partial rain situation on bushing surface in the absence and presence of booster shed.

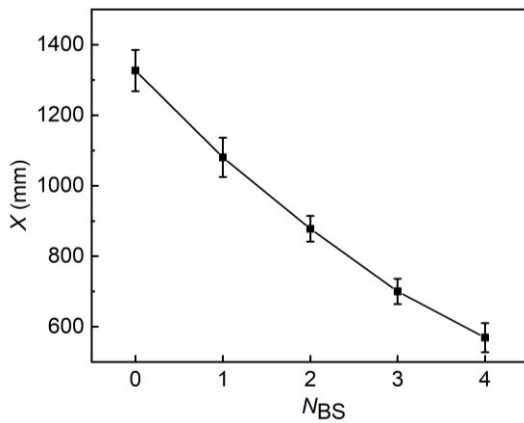


FIGURE 9. The effect of N_{BS} (the number of booster sheds) on X (the total length of water column).

In the enlarged part of Fig. 10, the points are marked as A-E where the significant rise of v emerges as 0-4 BS are installed, respectively. The length of the corresponding arc at that point is measured and defined as the critical length of arc (L_{arc}).

According to the determination of the critical length of arc, the measured results are listed in Table 4.

Based on the test results in Table 4, the relationship between L_{arc} and N_{BS} is obtained, as shown in Fig. 12.

In Figure 12, L_{arc} appears to grow with saturation as N_{BS} rises. It can be explained as follows:

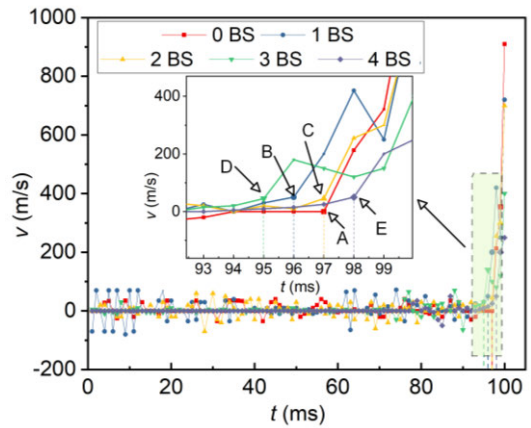


FIGURE 10. The arc propagation velocity (v). (A-E are the points where the significant rise of v emerges as 0-4 BS are installed, respectively. The flashovers occur at $t=100$ ms.)

TABLE 4. The results of arc characteristics test.

N_{BS}	L_{arc} (mm)	σ_L (%)	$L_{arc,m}$ (mm)	$f_{arc,mn}$	$f_{arc,m}$
0	1116.0	6.5	1116.0	0.469	0.469
1	1302.8	4.4	1302.8	0.620	0.620
2	1432.7	5.2	584.8	0.557	0.682
			847.9	0.808	
			461.7	0.660	
3	1542.6	4.2	516.7	0.738	0.734
			564.2	0.806	
			402.2	0.731	
			355.7	0.647	
4	1635.0	3.4	371.3	0.675	0.779
			505.8	0.920	

Notes: L_{arc} is the critical length of arc and σ_L is the relative standard deviation error of L_{arc} ; $L_{arc,m}$ is the length of local arc between two adjacent BS; Especially, $L_{arc,m}$ is equal to L_{arc} when N_{BS} is 0; $f_{arc,mn}$ is the ratio of $L_{arc,m}$ to l_m (l_m has been defined in the test arrangement); Especially when N_{BS} is 0, $f_{arc,mn}$ is the ratio of the critical length of arc to the insulation height h of the sample; $f_{arc,m}$ is the average of $f_{arc,mn}$.

From earlier study [32], the maximum electric field strength on the bushing surface appears on the booster shed edge. As a result, the arcs hang on the booster shed edges and almost develop synchronously as shown in Fig. 13, leading to the rising of L_{arc} . However, the spacing distance of booster sheds decreases with the increase of N_{BS} and the arcs are easy to bridge the adjacent booster sheds, which corresponds to the result that $f_{arc,m}$ continuously increases in Table 4. Consequently, the increase range of L_{arc} is falling with N_{BS} rising.

IV. DISCUSSION

A. EFFECT OF WATER COLUMN ON ELECTRIC FIELD

In order to study the effect of water column on the electric field, the electric field simulation was carried out for the sample without BS and with 1-4 BS. According to the test results in Table 3, the length of water column at the edge of shed in the simulation was determined.

The distribution of the electric field is shown in Fig. 14. Taking Fig. 14 (a), (b) and (c) as examples, the distribution

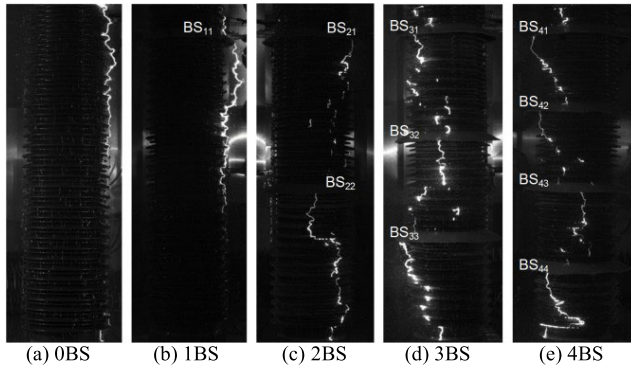


FIGURE 11. The critical arc propagation path. (Most of the partial arcs develop along the axial direction, and there is almost no partial arc on the surface of booster sheds).

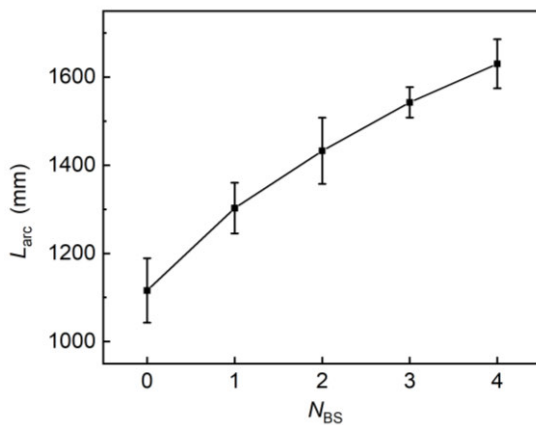


FIGURE 12. The effect of N_{BS} (the number of booster sheds) on L_{arc} (the critical length of arc).

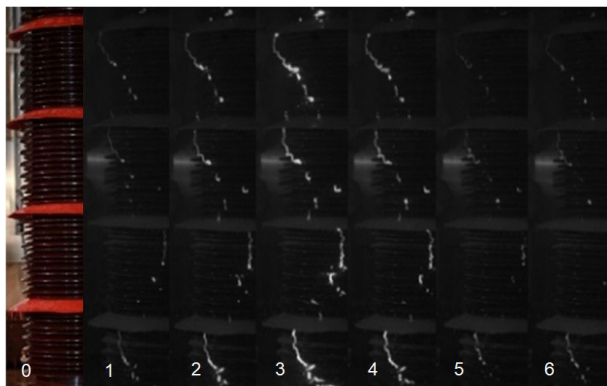


FIGURE 13. The synchronous propagation of the partial arcs on the sample with 4BS installed. (Photo 0 indicates the configuration and location of the actual sample. The time between two successive photos (Photo 1-6) is 50 ms.)

of the electric field strength (E) along the air gaps between the sheds from the top to the bottom of the sample is shown in Fig. 15. It can be seen from Fig. 14 and Fig. 15 that:

1) When there is no hanging water column on the surface of bushing without BS, the overall electric field strength is remarkably lower than that with water column. When the

sample is equipped without BS and with 1-4 BS in the presence of water column, respectively, the distribution of the electric field has no significant change on the whole.

2) Fig. 14 (g) shows that the electric field within the air gap between two adjacent sheds is obviously distorted by the water column, which is illustrated by the abrupt peaks in Fig. 15.

3) The maximum electric field strength occurs at the air-water interface at the end of water column. The electric field strength on the shed surface is far less than that within the air gap at the end of water column.

B. RELATIONSHIP BETWEEN X AND L_{arc}

Based on the test results in Table 2 and Table 3, the relationship between E_h and X can be obtained as shown in Fig. 16, which shows that E_h decreases as X increases, while there is not a linear relationship between them.

Form the test results in Tables 2 and 4, the relationship between E_h and L_{arc} is gained, as also shown in Fig. 16, where E_h rises with the increase of L_{arc} , yet not linearly.

It is worth mentioning that the two trends of E_h with the decrease of X and with the increase of L_{arc} are synchronous in Fig. 16, demonstrating a significant correlation between X and L_{arc} . According to Tables 3 and 4, the relationship between X and L_{arc} obtained by fitting is shown in Fig. 17 and equation 9, where the correlation coefficient R^2 is 0.9985.

$$L_{arc} = -0.68X + 2026.8 \quad (9)$$

Fig. 17 and equation (9) show that there is a remarkable negative correlation between X and L_{arc} . In order to explore whether there is such a relationship between surface rainwater characteristics and arc characteristics at the local position of the sample, the test results in Tables 3 and 4 are further analyzed.

The relationship between X_m and $L_{arc,m}$ can be obtained as shown in Fig. 18, where X_m is the total length of water column between two adjacent booster sheds and $L_{arc,m}$ is the length of local arc between two adjacent booster sheds when N_{BS} is m .

R^2 in Fig. 18 called correlation coefficient greater than 0.96 means there is an approximate negative correlation between the length of water column and the length of local arc at the local position of the sample, which is attributed to the effect of the electric field.

According to the simulation results, it can be inferred that the electric field strength along the shed surface is too low to promote the streamer development, whereas the electric field strength within the air gap at the end of water column is far greater due to the presence of water column, leading to the streamer discharge along the air gap. Besides, the water drop in the strong electric field will deform and then spray the charged particles at its tip, thus promoting the breakdown of air gap [22].

Therefore, when the applied voltage increases gradually, a local arc with higher energy will form in the air gap at the end of water column, which starts at the end of water column and develops to the upper surface edge of the shed below,

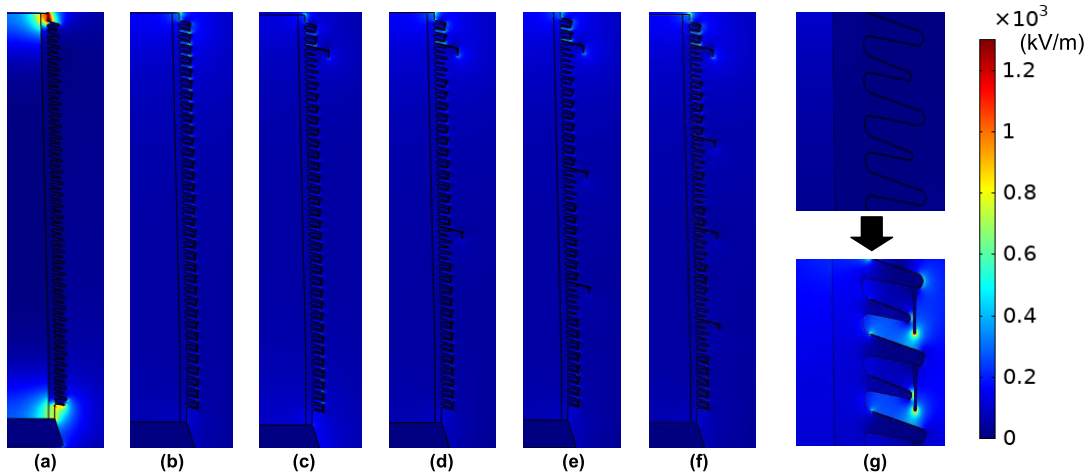


FIGURE 14. The distribution of the electric field. (a): without BS and water column; (b): without BS but with water column; (c): with 1 BS and water column; (d): with 2 BS and water column; (e): with 3 BS and water column; (f): with 4 BS and water column; (g): the comparison of electric field within the air gap with and without water column.

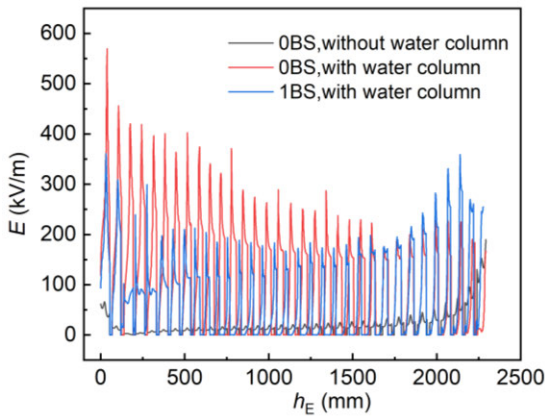


FIGURE 15. The distribution of the electric field strength (E) along the air gaps between sheds from the top to the bottom of the sample. (Take Fig. 14 (a), (b) and (c) as examples; h_E is the distance to the lower surface of the first shed).

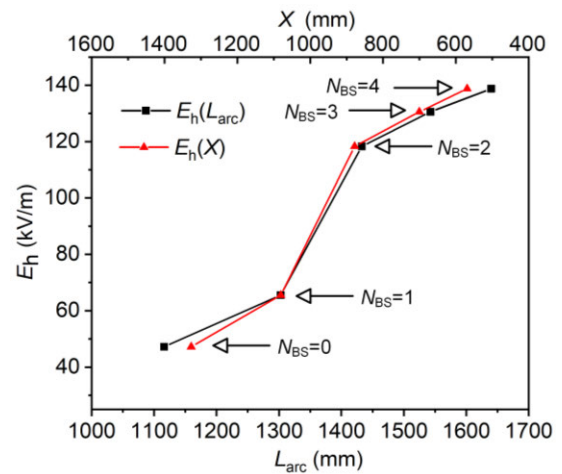


FIGURE 16. The effects of X (the total length of water column) and L_{arc} (the critical length of arc) on E_h (the rain flashover voltage gradient).

as shown in Fig. 3. The water column and the arc bridge two adjacent bushing sheds, and the longer the water column is, the smaller the arc length is. As a result, L_{arc} presents remarkable negative correlation to X_m , as well as L_{arc} to X .

C. EFFECT OF X ON E_h

Fig. 16 indicates that E_h increases with the decrease of X , the reason of which is discussed as the following.

Under the rain condition, the insulation task between the insulator sheds is mainly performed by the air gap, which bears most of the applied voltage [23]. As the water column between two adjacent sheds becomes shorter, the air gap at the end of the water column is longer and less likely to be broken down, which explains why E_h rises with the decrease of X .

Furthermore, the increase range of E_h rises in the beginning and then falls as X decreases in Fig. 16. When N_{BS} is one, E_h is higher than that without BS, but the rise of E_h is not

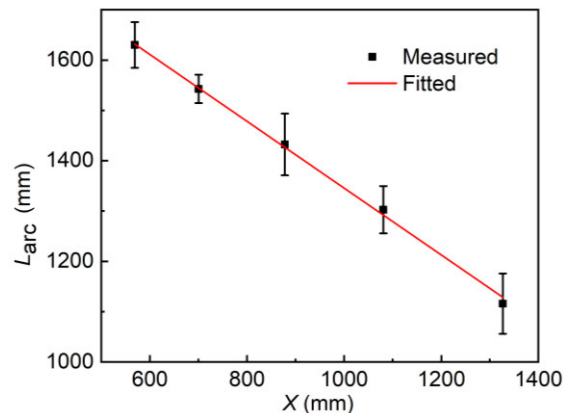


FIGURE 17. The relationship between X (the total length of water column) and L_{arc} (the critical length of arc).

remarkable. E_h has a sharp rise as N_{BS} is from one to two, whereas the rise of E_h gradually falls as N_{BS} exceeds two.

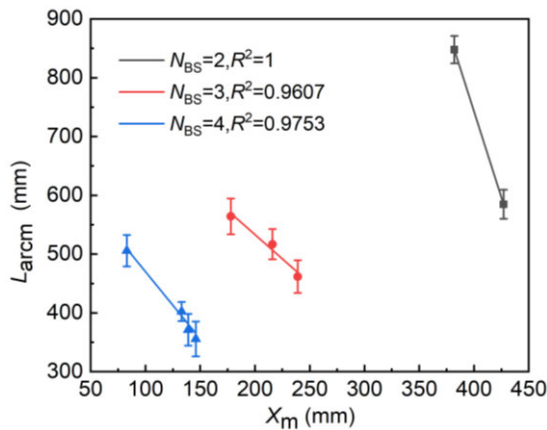


FIGURE 18. The relationship between X_m (the total length of water column between two adjacent BS) and L_{arc} (the length of local arc between two adjacent BS).

Based on the results in Table 3 and Fig. 7, the trend of curve $E_h(X)$ can be well explained as follows:

1) Compared with that without BS, X of the sample with only one booster shed (BS_{11}) is reduced. However, the length of water column (x_i) of the first several bushing sheds under BS_{11} is significantly smaller than that farther from BS_{11} , leading to relatively uneven wetting of the sample. As a result, E_h is higher than that without BS while the increase range of E_h is unremarkable.

2) X continuously decreases when two booster sheds (BS_{21} and BS_{22}) are installed. Moreover, x_9 - x_{19} under BS_{21} are not much different from x_{22} - x_{32} under BS_{22} , and the variations of x_i under BS_{21} and BS_{22} are approximately identical. The sample is equivalently divided into two units with similar surface rainwater characteristics, causing a more uniform wetting and an improved insulation performance of the sample on the whole. Moreover, according to [33] and [34], the local arc under BS_{21} causes an increase of voltage drop along the air gap between BS_{22} and the grounding end, and the air gap playing the role of a potential barrier prevents the re-equilibrium of the potential distribution, leading to a higher flashover voltage. E_h therefore increases significantly as N_{BS} is from one to two.

3) Simulation studies indicate that the higher N_{BS} is, the higher is resistance of the air gaps against voltage redistribution in the presence of the local arc, and the higher the final flashover voltage is [33], [34]. Although the sample is divided into three units with similar surface rainwater characteristics, the wetting uniformity of the sample is worse due to the increase of the dry bushing sheds without water column. Consequently, as N_{BS} is from two to three, E_h rises while its increase range falls, compared with that of two BS. In the same vein, there is the similar variation of E_h as N_{BS} is from three to four.

V. CONCLUSION

The following conclusions can be drawn:

1) The rain flashover voltages of the sample equipped with 1-4 BS are 39%, 150%, 176%, and 194% higher than that without BS, respectively, which indicates that BS can effectively improve the flashover performance of the sample under heavy rainfall.

2) As the number of booster sheds rises, the total length of water column decreases while the critical length of arc increases nonlinearly, however the both change ranges of them continually fall.

3) There is not only a remarkable negative correlation between the total length of water column and the critical length of arc on the whole sample but also on the local, which is attributed to the effect of the electric field.

4) The rain flashover voltage gradient along the insulation height is improved nonlinearly, and its increase range first rises and then falls with the total length of water column decreasing. It is not only because booster sheds divide the bushing into several units and lead to the changes of the wetting uniformity, but also the potential redistribution along air gaps varies in the presence of the local arc.

REFERENCES

- [1] W. McDermid and T. Black, "Experience with preventing external flashovers in HVDC converter stations," in *Proc. 17th Biennial IEEE Int. Symp. Electr. Insul.*, Jun. 2008, pp. 81–84.
- [2] F. A. M. Rizk and I. S. Kamel, "Modelling of HVDC wall bushing flashover in nonuniform rain," *IEEE Trans. Power Del.*, vol. 6, no. 4, pp. 1650–1658, Oct. 1991.
- [3] R. Hartings, "The AC-behavior of a hydrophilic and hydrophobic post insulator during rain," *IEEE Trans. Power Del.*, vol. 9, no. 3, pp. 1584–1592, Jul. 1994.
- [4] W. McDermid and T. Black, "External flashovers, related insulation failures and corrective measures in converter stations of Nelson river bipole 1 and bipole 2," *IEEE Trans. Dielectr. Electr. Insul.*, vol. 21, no. 6, pp. 2406–2414, Dec. 2014.
- [5] Y. Shen, W. T. Deng, Y. D. Zhang, and J. T. Quan, "Analysis and prevention treatment for rain flashover accident of ± 500 kV composite bushing," (in Chinese), *Insul. Surge Arrest.*, vol. 268, no. 6, pp. 16–21, Dec. 2015.
- [6] O. F. Orsino, A. C. Jose, R. Darcy, M. Rogerio, and G. C. Sylvia, "Use of booster sheds to improve performance of 800 kV multicone type insulators under heavy rain," *High Voltage Eng.*, vol. 37, no. 11, pp. 2772–2779, Nov. 2011.
- [7] X. Z. Yu, J. Zhou, S. Yokoi, K. Kondo, M. Maeda, and R. P. Huang, "Experimental study on improving the flashover characteristics of external insulation in UHV and UHV substations by umbrella," (in Chinese), *High Voltage Eng.*, vol. 39, no. 12, pp. 2980–2986, Dec. 2013.
- [8] C. Liu, Y. Zhu, J. Fang, C. Liu, and L. Wang, "Flashover performance of porcelain post insulator with full-clad booster shed," in *Proc. IEEE/PES Transmiss. Distrib. Conf. Expo. (T&D)*, Apr. 2018, pp. 81–84.
- [9] C. H. A. Ely, P. J. Lambeth, and J. S. T. Looms, "The booster shed: Prevention of flashover of polluted substation insulators in heavy wetting," *IEEE Trans. Power App. Syst.*, vol. PAS-97, no. 6, pp. 2187–2197, Nov. 1978.
- [10] P. J. Lambeth, "Laboratory tests to evaluate HVDC wall bushing performance in wet weather," *IEEE Trans. Power Del.*, vol. 5, no. 4, pp. 1782–1793, Nov. 1990.
- [11] X. Y. Xu, "Preventive treatment and analysis of the flashover on porcelain bushing of 500 kV substation equipments in rain," (in Chinese), *Power Syst. Technol.*, vol. 20, no. 6, pp. 5–8, Jun. 1996.
- [12] *Artificial Pollution Tests on High-Voltage Ceramic and Glass Insulators to be Used on a.c. Systems*, Standard IEC 60507, 2013.
- [13] *Application Guide of Auxiliary Silicone Rubber Shed for Transmission and Substation Equipment External Insulation*, (in Chinese), Standard DL/T 1469, 2015.

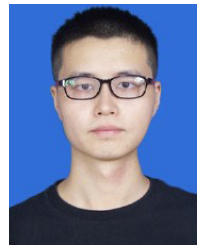
- [14] *Artificial Heavy Rain Test Method for High Voltage Bushing Under Pollution Condition*, (in Chinese), Standard DL/T 383, 2010.
- [15] Z. Zhang, X. Jiang, Y. Chao, L. Chen, C. Sun, and J. Hu, "Study on DC pollution flashover performance of various types of long string insulators under low atmospheric pressure conditions," *IEEE Trans. Power Del.*, vol. 25, no. 4, pp. 2132–2142, Oct. 2010.
- [16] J. D. Samakosh and M. Mirzaie, "Investigation and analysis of AC flashover voltage of SiR insulators under longitudinal and fan-shaped non-uniform pollutions," *Int. J. Elect. Power Energy Syst.*, vol. 108, pp. 382–391, Jun. 2019.
- [17] L. Yang, Y. Hao, L. Li, and Y. Zhao, "Comparison of pollution flashover performance of porcelain long rod, disc type, and composite UHVDC insulators at high altitudes," *IEEE Trans. Dielectr. Electr. Insul.*, vol. 19, no. 3, pp. 1053–1059, Jun. 2012.
- [18] L. Yang, Y. Hao, L. Li, and F. Zhang, "Artificial pollution flashover performance of porcelain long rod UHVDC insulators at high altitudes," *IEEE Trans. Dielectr. Electr. Insul.*, vol. 21, no. 4, pp. 1965–1971, Aug. 2014.
- [19] B. F. Hampton, "Flashover mechanism of polluted insulation," *Proc. IEE*, vol. 111, no. 5, pp. 985–990, May 1964.
- [20] C. Zhang, L. Wang, and Z. Guan, "Investigation of DC discharge behavior of polluted porcelain post insulator in artificial rain," *IEEE Trans. Dielectr. Electr. Insul.*, vol. 23, no. 1, pp. 331–338, Feb. 2016.
- [21] A. de la O and R. S. Gorur, "Flashover of contaminated nonceramic outdoor insulators in a wet atmosphere," *IEEE Trans. Dielectr. Electr. Insul.*, vol. 5, no. 6, pp. 814–823, Dec. 1998.
- [22] Y. Yuan, X. Jiang, S. M. Rowland, X. Cheng, and Q. Li, "Effect of water streams on the AC breakdown performance of short rod-plane air gaps," *IEEE Trans. Dielectr. Electr. Insul.*, vol. 21, no. 4, pp. 1747–1756, Aug. 2014.
- [23] J. Lu, P. Xie, and J. Hu, "AC flashover performance of 10 kV rod-plane air-gapped arresters under rain conditions," *Energies*, vol. 11, no. 6, pp. 1–11, Jun. 2018.
- [24] R. Courant, K. Friedrichs, and H. Lewy, "On the partial difference equations of mathematical physics," *IBM J. Res. Develop.*, vol. 11, no. 2, pp. 215–234, Mar. 1967.
- [25] Z. C. Guan, *Insulators and External Insulation of Transmission and Distribution Equipment*. Beijing, China: Tsinghua Univ. Press, (in Chinese), 2006.
- [26] L. C. Shu, X. H. Fan, and X. L. Jiang, "AC flashover calculation model of polluted suspension insulator," (in Chinese), *High Voltage Eng.*, vol. 36, no. 5, pp. 1077–1082, May 2010.
- [27] M. Slama, A. Beroual, and H. Hadi, "Analytical computation of discharge characteristic constants and critical parameters of flashover of polluted insulators," *IEEE Trans. Dielectr. Electr. Insul.*, vol. 17, no. 6, pp. 1764–1771, Dec. 2010.
- [28] D. Jolly, "Contamination flashover, part I: Theoretical aspects," *IEEE Trans. Power App. Syst.*, vol. PAS-91, no. 6, pp. 2437–2442, Nov. 1972.
- [29] S. Farokhi, M. Farzaneh, and I. Fofana, "Experimental investigation of the process of arc propagation over an ice surface," *IEEE Trans. Dielectr. Electr. Insul.*, vol. 17, no. 2, pp. 458–464, Apr. 2010.
- [30] S. Taheri, M. Farzaneh, and I. Fofana, "Electrical performance evaluation of EHV post insulators covered with ice under different air gap configurations," *IEEE Trans. Dielectr. Electr. Insul.*, vol. 21, no. 6, pp. 2619–2627, Dec. 2014.
- [31] J. Li, Z. Guan, L. Wang, H. Yang, and J. Zhou, "An experimental study of AC arc propagation over a contaminated surface," *IEEE Trans. Dielectr. Electr. Insul.*, vol. 19, no. 4, pp. 1360–1368, Aug. 2012.
- [32] Y. Yao, "The effect of booster shed on external insulation of 500 kV transformer high-voltage bushing under rain condition," (in Chinese), M.S. thesis, Dept. Elect. Eng., South China Univ. Technol, Guangzhou, China, 2019.
- [33] C. Volat and M. Farzaneh, "Three-dimensional modeling of potential and electric-field distributions along an EHV ceramic post insulator covered with ice—Part II: Effect of air gaps and partial arcs," *IEEE Trans. Power Del.*, vol. 20, no. 3, pp. 2014–2021, Jul. 2005.
- [34] S. M. Ale-Emran and M. Farzaneh, "Flashover performance of ice-covered post insulators with booster sheds using experiments and partial arc modeling," *IEEE Trans. Dielectr. Electr. Insul.*, vol. 23, no. 2, pp. 979–986, Apr. 2016.



LIN YANG (Member, IEEE) was born in Hunan, China, in 1984. He received the B.S. degree from Guangxi University, China, in 2007, and the Ph.D. degree from the South China University of Technology, China, in 2012. He is currently with the School of Electric Power, South China University of Technology, where he has been an Associate Professor since 2017. His research interests include HV outdoor insulation and on-line monitoring and the fault diagnosis of electrical equipment.



ZHIQIANG KUANG was born in Jiangxi, China, in 1996. He received the B.S. degree in electrical engineering from the Nanjing University of Science and Technology, China, in 2018. He is currently pursuing the M.S. degree with the South China University of Technology, China. His research interest includes HV outdoor insulation.



YIYE SUN was born in Anhui, China, in 1995. He received the B.S. degree in electrical engineering from the China University of Mining and Technology, China, in 2018. He is currently pursuing the M.S. degree with the South China University of Technology, China. His research interest includes HV outdoor insulation.



YIFAN LIAO was born in Jiangxi, China, in 1987. He received the M.Sc. degree from the School of Electrical Engineering, Wuhan University, China, in 2012. He is currently pursuing the Ph.D. degree with the South China University of Technology. He is also with the Electric Power Research Institute, China Southern Power Grid. His research interests include experimental research of HV technologies, HV engineering, and HV outdoor insulation.



YANPENG HAO (Member, IEEE) was born in Hebei, China, in 1974. She received the B.S. and Ph.D. degrees in electrical engineering from Xi'an Jiaotong University, China, in 1998 and 2003, respectively. She was a Postdoctoral Researcher with Tsinghua University, from 2003 to 2005. She is currently a Professor with the South China University of Technology, China. Her research interests include the condition perception and operation safety of transmission equipment, and atmospheric pressure dielectric barrier discharge.

Dr. Hao is the Leader of the High Voltage Group, SCUT. She is also a Commissioner of the Professional Committee on High Voltage and the Chinese Society for Electrical Engineering, a member of the Professional Committee on Engineering Dielectric, the China Electrotechnical Society, and the Executive Chairman of the 2nd IEEE International Conference on Electrical Materials and Power Equipment (ICEMPE), in 2019.



LICHENG LI was born in Jiangsu, China, in 1941. He received the B.S.E.E. degree from Tsinghua University, China, in 1967. From 1967 to 1980, he was with Gansu Electric Power Construction Corporation as a Chief Engineer. From 1980 to 1982, he was the Project Manager and a Principal Engineer of the China Extra-High Voltage Technology Company. He joined China Southern Power Company (the predecessor of China Southern Power Grid Company, CSG) in 1990, where he is currently a Secretary-General of the Consulting Group, CSG. He is currently a Professor with the South China University of Technology, China. His research interests include HVAC/HVDC transmission networks, paralleling system operation and stability, and wide-area measurement and control.



FUZENG ZHANG was born in Shandong, China, in 1979. He received the B.Sc. and M.Sc. degrees from the School of Automation, Northwestern Polytechnic University, China, in 2001 and 2004, respectively, and the Ph.D. degree from the Department of Electrical Engineering, Tsinghua University, Beijing, China, in 2008. He is currently with the Ultra-high Voltage Laboratory, Technology Research Center, China Southern Power Grid. His research interests include HV engineering and HV outdoor insulation.

• • •